"Radar-A-Thon" Concept Paper: RAPHAEL COTS Radar

Michael Woollard, Alan Bannon, Matthew Ritchie, Hugh Griffiths
Electronic and Electrical Engineering Department
University College London
London, WC1E 7JE
Email: michael.woollard.15@ucl.ac.uk

***Abstract*—This paper presents a low-cost X-band FMCW radar system suitable for short range sensing in an indoor environment. The design is based on a PLL-VCO architecture, and is realised as a direct conversion receiver. It can achieve range resolutions of $30\,\mathrm{cm}$ or $10\,\mathrm{cm}$ in standard and ultra-wideband modes respectively. The system is capable of producing programmable linear sweeps over wide bandwidths, and is compliant with FCC Part 15.**

I. Introduction

The "Radar-A-Thon" challenge requires a candidate radar system to sense multiple targets in a $20\,\mathrm{m}$ deep by $\approx 8\,\mathrm{m}$ wide scene hidden behind an RF-transparent curtain. The majority of these targets are stated to be canonical point scatters, such as corner reflectors. Both stationary and moving targets will be present. The stated aim of the challenge is to provide a description of the scene within the allocated sensing time. The radar unit used must be compliant with FCC Part 15 regulations, and have a total cost of <$750 for the maximal-value category.

II. Hardware design

The RAPHAEL system was originally conceived in 2018 as a low-equity, low SWAP-C synthetic aperture radar (SAR) unit for a UAV surveillance platform. The first prototype was designed and built at University College London by Bannon and Woollard as part of their final MEng project. The system operates in the X-band region, and can be programmed to generate complex linear-segmented frequency sweeps with optional phase modulation.

A. RF chain

A block diagram of the transceiver architecture is shown in Figure 1. Chirp generation is performed directly at X-band using a MAOC-009265 voltage-controlled oscillator (VCO) stabilised by a Texas Instruments LMX2492 fractional-N phase-locked loop (PLL). This device uses a $\Delta\Sigma$ architecture with a denominator size of 2^{24}. The LMX2492EVM evaluation module has been used as it is available off-the-shelf.

A PDW06399 two-way power splitter from Knowles Dielectric Labs is used to generate a reference signal for downconversion in the receiver chain, and another signal for amplification and transmission. It offers a nominal power split of $3\,\mathrm{dB}$ with an amplitude balance of $\pm 0.25\,\mathrm{dB}$ and phase balance of $\pm 5.0°$. An excess insertion loss of $0.25\,\mathrm{dB}$ and a return loss of $20\,\mathrm{dB}$ are achieved when the ports are matched to $50\,\Omega$.

TABLE I: MiniCircuits ceramic filter data

Part no.	Passband	Stopband (20 dB loss)	f_{co}	Insertion loss @ 10 GHz
HFCN-8400+	9 to 13 GHz	6 GHz	8.4 GHz	1.47 dB
LFCN-113+	0 to 10.8 GHz	14 GHz	12.25 GHz	0.97 dB

The HMC3653 low-noise amplifier is used to amplify both the local reference and received signal before the downconverting mixer. This device is an MMIC amplifier suitable for cascaded operation, providing $15\,\mathrm{dB}$ gain with a noise figure of $4.0\,\mathrm{dB}$. It is $50\,\Omega$ matched at both input and output ports, and is power via a single $5\,\mathrm{V}$ supply. The maximum output power is $15\,\mathrm{dBm}$ across the 7 to 15 GHz range, with a third-order intercept point of $28\,\mathrm{dBm}$ referred to input tones of $0\,\mathrm{dBm}$.

The HMC1056 mixer supports an output IF range of 0 to $4\,\mathrm{GHz}$; thus, the IF bandwidth is limited by the sampling rate of the digitising ADC. A software defined radio (SDR) is used to digitise the signal; if two phase-coherent channels are available, then the I/Q outputs of the mixer can be recorded on two input channels. Alternatively, a $90°$ hybrid combiner can be used to convert the mixer outputs to a single complex channel for recording. Low-cost SDRs such as the RTL-SDR have been tested with the system, although a final decision has not been made on the model that will be used in the competition.

Bandpass filters for the RF signal paths were constructed using discrete ceramic components obtained from MiniCircuits. The HFCN-8400+ high-pass filter and LFCN-113+ low-pass filter were chosen for this application, as they demonstrate good stopband attenuation with low excess insertion loss in the passband; they are also rated for up to 7 W RF input power. A brief summary of the components' characteristics is given in Table I.

B. Antenna

Following the design reported by Saponara and Neri for their X-band mobility surveillance radar [1], derived from [2], a Fabry-Perot cavity antenna was designed to provide a usable bandwidth of 8.6 to 12 GHz. The results presented in [2] have been independently reproduced, and the antenna characteristics

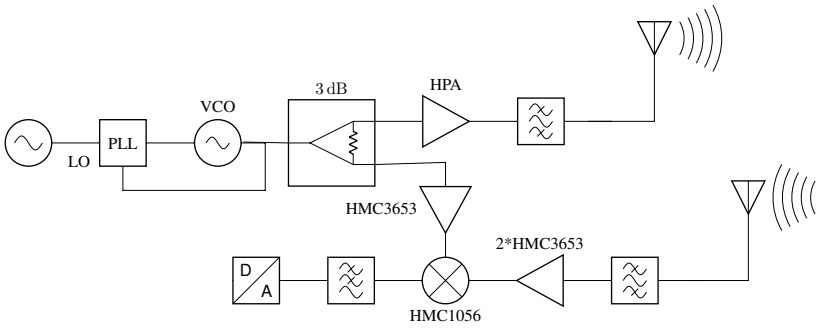

Fig. 1: A high-level block diagram of the proposed homodyne transceiver

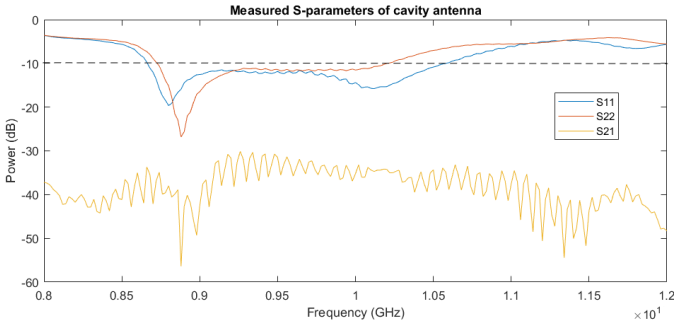

Fig. 2: Measured S-parameters for the cavity antenna

were investigated using the anechoic chamber facility at UCL. The measured S-parameters are shown in Figure 2. A gain of approximately 13 dBi is achieved across the operating band, with relatively little variation in the beamwidth.

C. Mechanical scanning system

A mechanically scanning system will be implemented to scan the target scene. A stepper motor will be used for motive force, connected via belt drive to a central rotating platform mounted on a single vertical axle. A rotary encoder will be used for positional data, and a six channel slip-ring to transmit power and data to the platform will allow continuous rotation. Placing the encoder directly on the central axle will remove any effects of mechanical backlash from the rest of the system and allows full closed-loop control.

All components in the system are common sizes and specifications to simplify procurement and assembly. All axles will be 10 mm diameter to allow the use of standard bearings, belt pulleys, encoders, and slip-rings. GT2 timing belts and pulleys will be used due to their high availability and low backlash.

The scanning system will allow precision pointing in $< 0.6°$ increments without considering microstepping. With microstepping, the system could achieve at least an order of magnitude improvement on this performance. The system will provide the option to scan quickly and continually allowing a picture of the scene to be very rapidly generated, while also allowing pointing and tracking of targets of interest within the scene.

TABLE II: Bill of materials for core RF chain

Part	Cost	Source	Quantity	Total
LMX2492EVM	£264.75	Mouser (UK)	1	£264.75
HMC1056	£25.60	Mouser (UK)	1	£25.60
HMC3653	£20.00	Mouser (UK)	3	£60.00
HFCN-8400+	$3.25	Mini-Circuits	2	$6.50
LFCN-113+	$2.25	Mini-Circuits	2	$4.50
PDW06399	£11.58	Mouser (UK)	1	£11.58

To interface with the rest of the system, the scanning system will use a simple serial UART connection to accept movement parameters and position targets from the REDHAWK controller software (see Subsection III-D).

D. Waveform design and adaptation

The LMX2492 is capable of producing chirps with up to 8 programmable linear sections. The settings can be modified during operation via a serial port interface over USB, allowing for adaptive waveform generation. Binary phase-shift keying can be implemented, but has been disabled for the competition configuration as the radar will not be operating in a contested environment.

E. Bill of materials

A cost breakdown for the core RF chain is given in Table II. It should be noted that a considerable cost saving may be achieved by reproducing the LMX2492 board and purchasing the components separately; however, this would reduce the COTS appeal of the system. A full bill of materials will be provided at the time of competition, reflecting the state of the system as used during the competition. This will include the costs of all components and other parts, such as PCB substrate materials.

III. Signal Processing

A. Range profile generation

The sampled baseband data from the SDR is comprised of a set of beat frequencies corresponding to the target ranges (and any associated Doppler shift), which is the fundamental operating principle of linear FMCW radars. Taking the FFT of the sampled beat frequency vector yields a single raw range profile. These profiles are accumulated into a buffer over a coherent integration interval; the result is then stored in a

slow-time matrix of profiles which can be further processed to identify moving targets.

B. Moving targets

Two primary methods will be used for the detection of moving targets in the scene. A Moving Target Indicator (MTI) filter will be applied to the range profile series obtained, with moving targets identified by detected peaks in the output map. Good results have previously been obtained with a simple three-pulse canceller, as shown in Section IV.

The chirp generator will also be configured to transmit a waveform containing alternate up-/down-chirps. This will cause the target to display paired responses at two frequencies, the lower notated as f_{bd} and the higher by f_{bu}, due to the Doppler shift imparted to the received waveform by the target's motion. The radial velocity v_r can be calculated from Equation 1. Identifying these peaks in the real-time display will permit the isolation of moving targets and provide an estimate of their velocity.

$$v_r = \frac{\lambda_0}{4}(f_{bd} - f_{bu}) \tag{1}$$

C. Angular separation of targets

As the system only contains a single receive element, mechanical steering of the beam is required to resolve targets in azimuth. Mechanical scanning of the system using the process described in Subsection II-C will yield a time-series of range profiles which can be associated with the azimuth angle at which they were sampled. Corrections for the antenna pattern will be applied to aid in identifying targets on the real-time display. Where moving targets require further characterisation, a restricted angular scan function will be available to track the target during its motion.

D. Software implementation

The REDHAWK SDR framework [3] will be used to process data from the radar unit. This allows the processing chain to be made agnostic to the SDR and computational hardware used throughout the development process. Pre-built "waveforms" will be constructed to encapsulate the anticipated post-processing required. Should further modifications be necessary during the competition, this can easily be accomplished through the Chalkboard interface provided by the Eclipse-based IDE for the REDHAWK framework.

IV. Performance Demonstration

Figure 3 shows the data captured for a trial run conducted in the Wilkins courtyard at UCL. A subject holding a corner reflector walked away from the radar, pausing at three locations marked by square stools, before walking back towards the radar in the same fashion. The strong response from the back wall of the enclosed courtyard is visible at 30 m, and numerous other strong returns are observed from stationary objects such as the stools. The MTI processing clearly suppresses the stationary returns, highlighting the moving target.

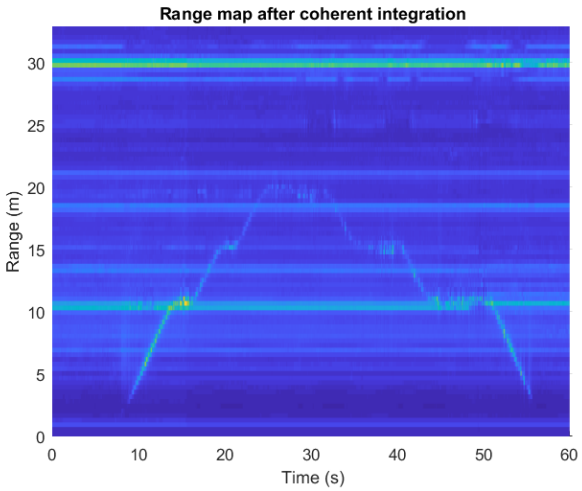

(a) Range profiles after coherent integration

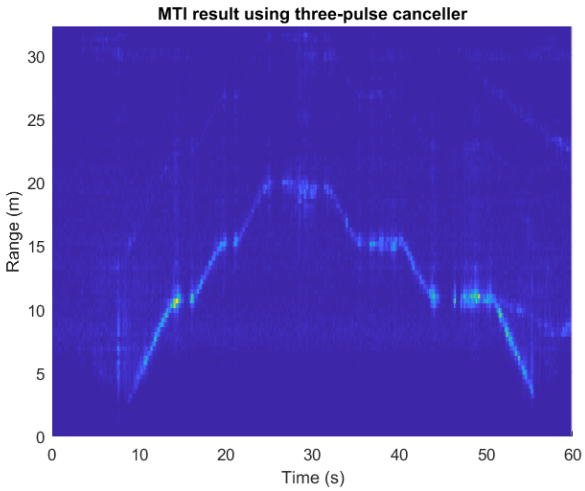

(b) MTI display after three-pulse canceller

Fig. 3: MTI result for the corner reflector test in the Wilkins courtyard at UCL

A similar experiment was conducted in front of Birkbeck College facing the north wall of Senate House. The results are shown in Figure 4. This data capture was synchronised with a video recording of the scene to help match tracks to the associated targets. The pedestrians in this experiment were not carrying corner reflectors; the strong target at 20 m was a bin which was obscured by pedestrians walking in front of it, leading to a flash in the MTI display.

V. FCC Compliance

To be eligible for competition entry, the system will comply with the FCC Part 15 legislation. As an intentional radiator, it is required to abide by the provision of Part 15 Subsection C.

A. System design and operation

If the full available bandwidth is used, the device is an intentional radiator operating in an ultra-wideband configuration, as set out in Subpart F. It is a through-wall imaging system

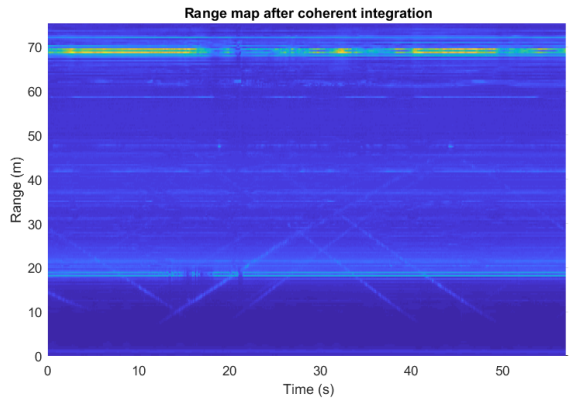

(a) Range profiles after coherent integration

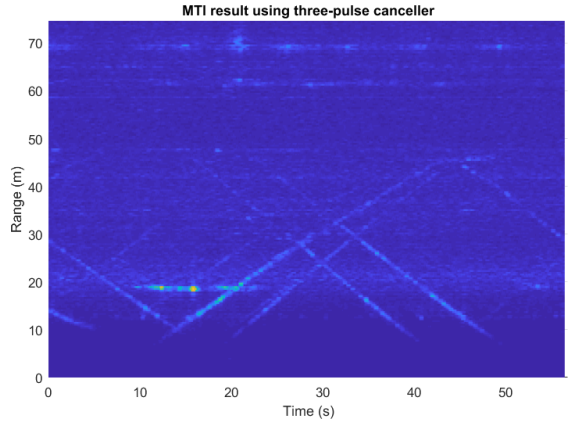

(b) MTI display after three-pulse canceller

Fig. 4: MTI result for the film-synchronised data capture

as defined by §15.503(i), but not a through D-wall imaging system; it is **not** subject to §15.510. §15.205(d)(6) exempts such devices from the restricted operating band requirements of §15.205.

As set out in §15.525, coordination through the FCC is required before a UWB imaging system can be used.

Should permission for ultra-wideband operation be refused, the unit will instead be operated in the 9.5 to 10.6 GHz band, as the neighbouring bands are restricted under §15.205. In this case, the device would not be subject to Subpart F of the FCC Part 15 regulations, as the bandwidth would be less than 500 MHz and the fractional bandwidth, as given by Equation 2, would be < 0.2. Instead, it would be subject to §15.205.

The unit is considered a "home-built device" under §15.23, and is therefore exempt from certification requirements. To comply with §15.203, the SMA connectors have been permanently attached with "Loctite" to prevent an unauthorised antenna being connected. This is in compliance with official guidance as published in KDB Publication 353028 (see §2(b)(ii)(1)).

$$B_{frac} = \frac{2(f_H - f_L)}{f_H + f_L} \tag{2}$$

TABLE III: Radiated emission limits for indoor ultrawideband operation

Frequency in MHz	EIRP in dBm
960-1610	-75.3
1610-1990	-53.3
1990-3100	-41.3
3100-10600	-41.3
Above 10600	-51.3

B. Transmitted power levels

If not operating in the ultrawideband mode, the maximum in-band emitted field strength is $500\,\mu\mathrm{V\,m^{-1}}$ at a distance of 3 m. This is specified by §15.209. §15.245 places additional limits on the field strength of harmonics that may be emitted in the 10 500 to 10 550 MHz band.

As the system will be mains-powered, it would be an indoor UWB system as detailed in §15.517 when operating in UWB mode. The radiated power is limited by §15.517(c) and (d) to the EIRP limits shown in Table III.

C. Out-of-band emissions

The largest source of potential out-of-band emissions in the system is the chirp generator, where spurs can be generated through numerous mechanisms. Fractional dithering is enabled on the LMX2492 to reduce the power present in fractional spurs. The additional noise introduced does not have a significant impact on system performance as the transceiver has a direct downconversion receiver (DCR) architecture. In addition, a third-order loop filter is used to suppress spurious signals in the feedback path.

A bandpass filter has been included at the RF output before transmission to ensure that the emitted signal is restricted to the operating band. The antenna also restricts the out-of-band emissions, as the passband of the double FSS that forms the front-plane is set to reject signals outside the useful operating range of the radar.

VI. Conclusions and Future Work

A design for a low-cost COTS radar suitable for tackling the "Radar-A-Thon" challenge has been presented. Successful operation of an earlier prototype has been demonstrated, and the required changes to ensure compliance with FCC Part 15 have been identified. A full specification of the system as presented at the competition will be made available to the judges at the time, along with the measured emissions spectrum and a cost breakdown to prove eligibility for the maximal-value category.

References

[1] S. Saponara and B. Neri, "Design of compact and low-power x-band radar for mobility surveillance applications," *Computers & Electrical Engineering*, vol. 56, pp. 46–63, 2016.

[2] N. Wang, Q. Liu, C. Wu, L. Talbi, Q. Zeng, and J. Xu, "Wideband fabry-perot resonator antenna with two complementary fss layers," *IEEE Transactions on Antennas and Propagation*, vol. 62, no. 5, pp. 2463–2471, 2014.

[3] "REDHAWK SDR Framework." [Online]. Available: https://redhawksdr.github.io/